Biosensors and Bioelectronics 24 (2009) 2528–2533

Contents lists available at ScienceDirect

Biosensors and Bioelectronics

journal homepage: www.elsevier.com/locate/bios

SOI optical microring resonator with poly(ethylene glycol) polymer brush for label-free biosensor applications

Katrien De Vos[a,*], Jordi Girones[b], Stepan Popelka[c], Etienne Schacht[b], Roel Baets[a], Peter Bienstman[a]

[a] Photonics Research Group, Department of Information Technology, Ghent University – IMEC, Sint-Pietersnieuwstraat 41, B-9000 Gent, Belgium
[b] Polymer Material Research Group, Ghent University, Krijgslaan 281, B-9000 Gent, Belgium
[c] Institute of Macromolecular Chemistry, Academy of Sciences of the Czech Republic, Heyrovskeho namesti 2, 16206 Praha 6, Czech Republic

ARTICLE INFO

Article history:
Received 11 October 2008
Received in revised form 18 December 2008
Accepted 5 January 2009
Available online 14 January 2009

Keywords:
Silicon-on-Insulator
Microring resonator
Optical biosensor
SAM
Non-specific binding reduction
Label-free biosensor

ABSTRACT

Label-free monitoring of biomolecular interactions has become of key importance for the emerging proteomics field. Monitoring real time interaction kinetics and high throughput screening of complex samples is of major importance for a variety of applications. We previously reported the use of Silicon-on-Insulator photonics microring resonators for cheap disposable biosensors on chip. Silicon photonics is a platform for micro- and nanoscale integrated devices that can be fabricated at extremely low cost, with standard CMOS processing facilities. Incorporation of a hydrophilic heterobifunctional polymer coating on the silicon chips largely improved the system's response to non-specific binding. We report the chemical coating procedure, the chemical surface characterization and optical measurements for both specific and non-specific interactions. Two heterobifunctional polymer coatings were investigated, α-sulfanyl-ω-carboxy-poly(ethylene glycol) and monoprotected diamino-poly(ethylene glycol). Homogenous coatings with thicknesses of 2.3 and 2.5 nm were obtained, corresponding to a surface loading of 99 pm/cm^2 carboxy- and 97 pm/cm^2 aminogroups, respectively. The polymer coated sensor with covalently bound biotin receptor molecules showed very low response to Bovine Serum Albumin (BSA) up to 1 mg/ml in contrast to a high response to avidin with much lower concentrations (2, 10, 87.5 and 175 μg/ml). By extrapolation the detection limit is about 10 ng/ml or 0.37 fg avidin mass. Comparison with the values reported for standard silanization confirms the polymer coating does not deteriorate the system's limit of detection. This makes the optical biosensor chip suitable to be integrated in a microflow system for commercial label-free biosensors and for lab-on-a-chip applications.

1. Introduction

Label-free biosensing with optical microcavities is considered to be a very promising technique due to its high sensitivity and its potential for integration in multidimensional arrays (Vollmer and Arnold, 2008; Fan et al., 2008). A binding event in the near vicinity of an optical cavity will change the local refractive index, which results in a change in the effective refractive index of the optical mode and hence in a resonance wavelength shift. In contrast to other phase change interrogation techniques such as interferometers, in an optical cavity light interacts multiple times with the assay. The increased photon lifetime in an optical cavity results in sharp resonance peaks when converted to the frequency domain, enabling the detection of ultra small changes of the resonance wavelength. This direct signal is a quantitative measure for the number of binding events. Unlike the response signal of interferometers, the response of optical cavities does not decrease with decreasing sensing area. Thus, tens of sensors can be placed on a square millimeter without loss of sensitivity. However, addressing extremely small sensors with molecules is a challenging fluidic problem that might ask for novel concepts. Commercial tools exist to spot proteins down to 5 μm spot size, although they have not been widely used so far. Unlike free space optical biosensors, integrated biosensors have virtually no limitations for multiplexing. There is no risk of optical signal interference from different sensing spots thanks to the independent read out, for example through vertical grating couplers as described in this manuscript (see Section 2.3).

While labeled detection methods can be sensitive down to a single molecule (Moerner, 2007), labels can structurally and functionally alter the assay and the labeling process is labor intensive and costly. Quantification is difficult since the bias label intensity level is dependent on all working conditions (Yu et al., 2006). Direct biosensors overcome specificity, reliability and durability problems induced by labels. Detection is done in real-time, which is important for kinetic interaction studies and point-of-care diagnostics. Since the concept was first described, over 100 papers have

* Corresponding author. Tel.: +32 9 264 89 30; fax: +32 9 264 35 93.
E-mail address: Katrien.Devos@intec.ugent.be (K. De Vos).

0956-5663/$ – see front matter © 2009 Elsevier B.V. All rights reserved.
doi:10.1016/j.bios.2009.01.009

been published on optical cavities for various sensing applications, even showing single molecule detection (Armani et al., 2007). Planar microring resonators are promising implementations of optical cavities for biosensing, because of the mass production possibilities using replica molding or photolithography. Chao et al. showed biomolecular detection with planar polymer microring resonators, fabricated by a direct imprinting technique, with a detection limit of 250 pg/mm^2 (Chao and Guo, 2006). Recently Ramachandran et al. applied a planar glass-based microring array in which 5 microrings were sequentially scanned for rapid detection of whole bacterial cells, proteins and nucleic acids (Ramachandran et al., 2008). The material system used in this work, Silicon-on-Insulator (SOI), in contrast to glasses or polymers, allows the reuse of standard high quality CMOS processing facilities, in particular 193 nm lithography, for fabrication of photonics micro- and nanodevices (Bogaerts et al., 2005). This opens the route for very cheap, potentially disposable devices. Thanks to the high contrast between the refractive indexes of silicon (3.47) and silicon dioxide (1.44) SOI is suitable for the fabrication of micron- and submicron sized optical cavities of very high quality. This is a major advantage since the smaller the cavity, the less molecules are needed to cover its entire surface, and as mentioned, the response does not decrease with decreasing surface area (De Vos et al., 2007; Densmore et al., 2008). For this reason we tend to refer to total mass coverage as a figure of merit for detection limit rather than surface coverage per area, but both values are reported. The combination of low cost fabrication and high sensitivity through small dimensions makes SOI a good candidate for disposable biosensor array chips.

The properties of a biosensor critically depend on the quality of the interfacial layer, especially for detection in complex samples. The interfacial layer has to allow immobilization of receptor molecules and at the same time effectively block non-specific interactions with the macromolecular components of the analyzed sample. In addition it must be stable, must not affect the sensor's sensitivity and must not hinder transport of the chemical or biological compounds to the surface. So homogenous and thin layers are required. Straightforward surface coatings of silicon are based on assemblies of silane reagents that can bear a wide range of functional groups for receptor molecule immobilization. However, the coatings of low molecular silanes typically do not have sufficient resistance to non-specific adsorption. This can be improved by attaching an ultra thin layer of a hydrophilic polymer like poly(ethylene glycol) (PEG). The ability of PEG layers to reduce non-specific interactions in various detection systems is well documented (Unsworth et al., 2007; Norde and Gage, 2004). The PEG layer can be introduced in a single step, by using PEG bearing alkoxysilane end-groups (Bluemmel et al., 2007; Andruzzi et al., 2005), or in two steps when a primary adhesion layer is firstly applied, e.g. silane layer containing epoxy groups followed by coupling of PEG with reactive terminal groups such as diamino-PEG (Piehler et al., 2000; Wolter et al., 2007; Proll et al., 2005). However, possible attachment to the surface through both terminal groups would decrease the concentration of free functional groups intended for immobilization of receptor molecules. Therefore, instead of homobifunctional PEGs we examined two heterobifunctional PEGs with functional end-groups of very different reactivity towards epoxides. α-sulfanyl-ω-carboxy PEG (HS–PEG–COOH) and monoprotected diamino-PEG (H_2N–PEG–NH-Boc) allowed the introduction of reactive carboxy and amino groups on the surface of the SOI microring, respectively. The functionalization procedure was characterized by ellipsometry, confocal microscopy, dark field optical microscopy and X-ray Photoelectron Spectroscopy. The high affinity system avidin/biotin and bovine serum albumin (BSA) have been used to perform specific and non-specific binding tests. Although avidin/biotin will not be the ultimate biological system studied with these biosensor chips, it is a useful model affinity couple to demonstrate the feasibility and reproducibility of the detection. It also allowed us to characterize the sensitivity of the system and to show the efficiency of the PEG coatings to reduce non-specific interactions. To our knowledge it is the first time PEG brushes have been successfully applied to structured silicon waveguides for label-free optical on chip biosensing.

The paper is structured as follows; chemical and optical methods and characterization techniques are described in Section 2. Results of the chemical characterization of the PEG coatings are discussed in paragraph 3. Section 4 describes and comments on the optical experiments.

2. Experimental

2.1. Materials and methods

3-(Glycidyloxypropyl)trimethoxysilane (GOPTS) was purchased from Aldrich. Iso-propanol, acetone, toluene and dimethylformamide (DMF) were obtained from Acros and from Sigma–Aldrich. Except for toluene, which was dried over calcium chloride, all chemicals were used as received. Phosphate-buffered saline (PBS: 10 mM, pH 7.4, 125 mM NaCl) was prepared from sodium phosphate mono- and dibasic salts purchased from Aldrich. Heterobifunctional PEGs, α-sulfanyl-ω-carboxi poly(ethylene glycol) (HS–PEG–COOH) and α-tert-butyloxycarbonylamino-ω-amino-poly(ethylene glycol) (H_2N–PEG–NH–Boc) were purchased from RAPP Polymere, Tubingen/Germany. The dye for the fluorescence tests was AlexaFluor® 555 cadaverine (Invitrogen). 1-Ethyl-3-(3-dimethylamino-propyl)carbodiimide (EDC), N-hydroxysuccinimide (NHS), avidin and bovine serum albumin were acquired from Sigma–Aldrich. EZ-Link® biotinylation reagents (NHS-LC-biotin and 5-(biotinamido)-pentylamine) were purchased from Pierce.

Polished single-crystal silicon wafers that were used as model substrates for the characterization of the polymer layers (Section 2.2). The substrates were first cleaned in an ultrasonic bath in iso-propanol and acetone, 10 min each. After the wet cleaning process, samples were blown dried with argon and the surfaces were activated with low pressure oxygen plasma for 10 min using a Femto plasma generator (Diener Electronics) operating at 100 W and 0.5 mbar. After cleaning and activation, the sample slides were tested for small contact angles (<5°). Activated substrates were immediately immersed in freshly prepared solutions of GOPTS in toluene (1%, w/w) and incubated overnight at room temperature. Unbound material was removed by successive sonication in pure toluene and acetone. Finally, the substrates were cured in a vacuum oven for 1 h at 100 °C.

HS–PEG–COOH and H_2N–PEG–NH–Boc layers were deposited from 3 mg/ml solutions in acetone. 100 μl of the PEG solutions were deposited on the surface of each substrate in 20 μl portions to allow solvent evaporation. The specimens were subsequently placed in a vacuum oven at 90 °C for 40 h in order to enable the end groups to anchor to the epoxy-silane layer. Unbound PEG was removed by rinsing multiple times with milliQ water in an ultrasonic bath.

For the biotinylation of GOPTS treated substrates described in the experiment (Section 4), 100 μl of EZ-Link 5-(biotinamido) pentylamine in DMF (2 mg/ml) was added to substrates immersed in 2 ml of PBS each. The reaction proceeded overnight at room temperature. The carboxy groups from substrates treated with HS–PEG–COOH were activated by immersing the substrates for 30 min in a NHS/EDC solution (0.1 M/0.4 M). After rinsing with MilliQ water, the activated samples were immersed for 2 h in 2 ml PBS to which 100 μl of EZ-Link 5-(biotinamido) pentylamine (2 mg/ml) was added. Release of the Boc groups in substrates coated with H_2N–PEG–NH–Boc was accomplished by immersing the substrates in trifluoroacetic acid (TFA) for 10 min. After rinsing

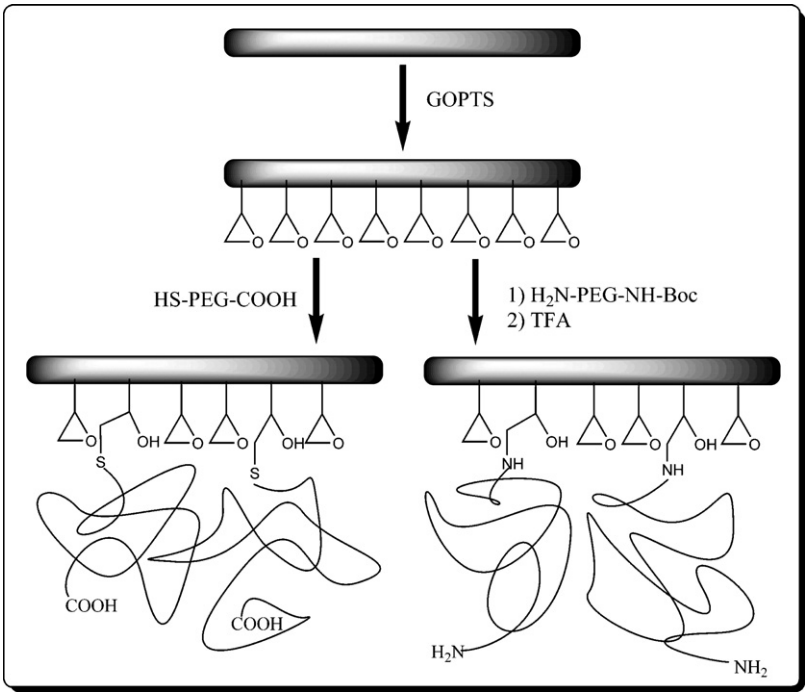

Fig. 1. The chemical reactions applied for the coating of silicon surfaces (thicknesses of the different layers are not to scale).

with MilliQ water and PBS, chips were immersed in 2 ml PBS, followed by the addition of 100 μl of EZ-Link biotin-LC-NHS in DMF (2 mg/ml). Reaction proceeded for 2 h at room temperature. After biotin coupling, all samples were rinsed with PBS and sonicated successively in PBS and MilliQ water. The chemical reactions applied for the coating of silicon surfaces are schematically depicted in Fig. 1.

2.2. Surface characterization methods

Structured SOI samples and bare silicon wafers were treated in parallel. Bare silicon surfaces were examined by static and dynamic contact angle using the drop shape analysis apparatus OCA 20 from Dataphysics. For static contact angle, a 2-μl MilliQ water droplet was placed on the surface of the sample and imaged using a video camera. At least three measurements per sample were performed; results from two to five samples were averaged. For dynamic contact angle measurements, 5 μl MilliQ water was added to a 2-μl drop at 0.5 ml/min.

The thicknesses of the GOPTS and PEG layers were determined by means of an M-2000FI Spectroscopic Ellipsometer (J.A. Woollam) at an angle of incidence of 75°. Ellipsometric data were acquired and evaluated by Complete EASE software (J.A. Woollam Inc.). The optical model of the multilayered substrates consisted of the software built-in optical functions of silicon, native silicon oxide and thermal silicon oxide (Herzinger et al., 1998). Optical constants of silicon oxide were also used for GOPTS layer. The index of refraction of PEG layer was modeled by a Cauchy dispersion function $A_n + B_n/\lambda^2$ (Tompkins and McGahan, 1999) and extinction coefficient was taken to be zero since this polymer is a dielectric with negligible absorption in the UV–vis range used in the measurement. The Cauchy parameters $A_n = 1.5$ and $B_n = 0.0059\ \mu m^2$ were obtained from a simultaneous fit for thickness, A_n and B_n of ellipsometric data acquired from an auxiliary PEO layer (ca. 100 nm thick), spin cast on a bare silicon wafer.

The bare silicon samples were analyzed by XPS using a Fissions S-probe apparatus provided with a fine focus Al–K source with a quartz monochromator.

Although parallel treatment of structured and bare wafers for chemical characterization is a commonly used approach, to confirm the actual presence of functional groups on the waveguides we analyzed the structured samples by confocal fluorescence microscopy. Fluorescence tests were performed with a confocal Carl Zeiss LSM 510 microscope equipped with an argon laser module (Carl Zeiss Inc., Thornwood, NY) using a 10 × 0.25-na objective. Fluorophores were excited at 543 nm with a HeNe laser.

2.3. Optical transducer

Microring resonators are processed on SOI wafers, using 193 nm deep UV-lithography and dry-etching (Bogaerts et al., 2005; Selvaraja et al., 2008). The high index contrast platform enables design of compact and high density circuits. However, this sets high demands for the fabrication technology, since the spectral characteristics of nano- and microdevices are extremely sensitive to dimensional variations down to a few nanometers. Advanced CMOS fabrication processes are adapted to fabrication of photonics circuits to obtain such high resolution and extreme stability. The microresonators used in the experiments are racetracks with radius 5 μm and straight sections of 2 μm for good coupling control (Fig. 2B). The waveguide dimensions are 220 nm × 450 nm (Fig. 2A). The resonators have a quality factor of 20,000 and a finesse of 240. In the time domain, a high internal Q-factor corresponds to a long photon life time in the cavity, and hence to an increased light-matter interaction. Transformed to the frequency domain, this corresponds to small resonance peaks, so small shifts can be distinguished. Moreover, a high Q-factor makes the sensor less sensitive to noise. When measuring intensity changes at a fixed wavelength, the response scales with the Q-factor. The intensity measurement scheme is beneficial if detecting extremely small amounts of analyte, but the dynamic range is restricted by the extinction of the resonance peak. The ultimate limit of detection, whether measuring wavelength shifts or intensity shifts, is equal to the ratio of sensor resolution and sensor sensitivity (White and Fan, 2008). The sensor resolution on the resonance peak shift for the described experiments is 2 pm. It is limited by various factors; the original

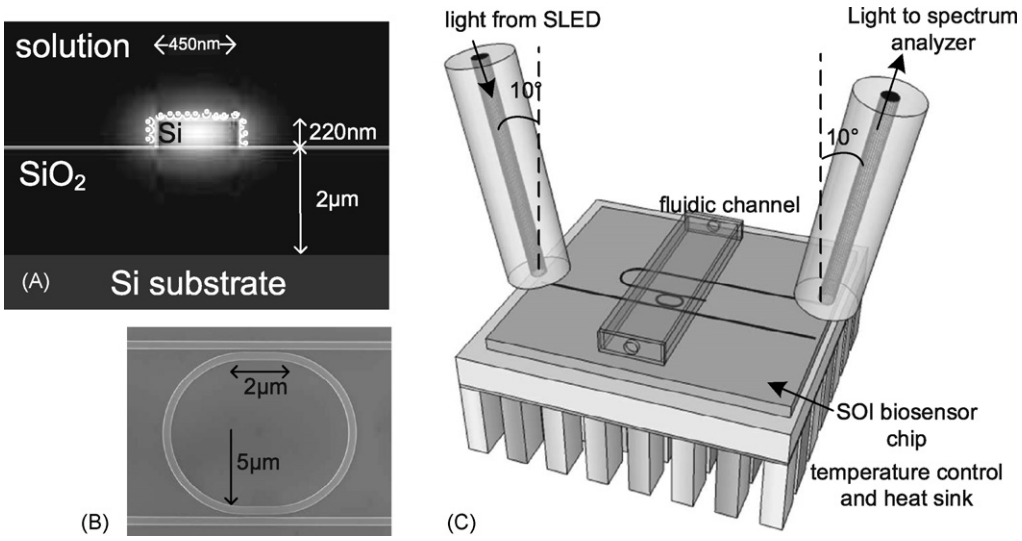

Fig. 2. (A) SOI waveguide for evanescent field biosensing (not to scale), (B) SEM picture of an SOI racetrack resonator with radius 5 μm and straight sections 2 μm, (C) Illustration of measurement setup.

signal quality defined by Q-factor, extinction ratio and equipment noise, the fitting quality and the resonance wavelength stability in time. The latter can be influenced by temperature, flow conditions or other environmental parameters. We keep in mind that high Q-factors set high demands to the resolution of the read-out equipment and that the Q-factor is related to the physical size of the resonator. By increasing the ring's radius, the Q-factor will increase. 20,000 is a value that holds a good compromise between small surface area, small peak width and maximal extinction (critical coupling). The finesse is defined as the ratio of the free spectral range and the peak width. A high finesse is important when making series of ring resonators in a bus waveguide configuration for multiarray sensing. It avoids spectral overlap between resonators with slightly different dimensions and hence reduces possible cross-talk. Light is coupled from a single mode waveguide at 10° from the vertical to the waveguides on the chip through grating couplers. This enables high alignment tolerances (Bogaerts et al., 2005). The shallow etched gratings have maximal coupling efficiency of 31% at 1.55 μm wavelength (40 nm 1 dB bandwidth). All measurements are performed with a superluminescent LED and an optical spectrum analyser (Agilent 86140B). Spectral scans are stored every 3 seconds. After fitting the data to a Lorentzian curve, the resonance wavelength is plotted versus time. A flow cell is mounted on top of the chip, connected through tubings with a Harvard syringe pump for controlled fluid delivery (Fig. 2C). The entire system is placed on a temperature stabilized chuck to avoid thermally induced signal drift.

3. Surface characterization results

3.1. GOPTS deposition on substrates

The deposition of the GOPTS layer was confirmed by ellipsometry, contact angle and XPS on model Si/SiO_2 substrates (see Table 1). Reproducible thicknesses of 1.3 ± 0.3 nm are obtained. After GOPTS treatment, the characteristic presence of 2 peaks at 284.7 eV and 286.4 eV, corresponding to C–C/C–H and the C–O bonds, respectively, was observed on the high-resolution XPS spectra of carbon (C1s). Si/SiO_2 wafers with smooth monolayers presented a static contact angle of $53° \pm 2°$, in good agreement with previously reported values (Luzinov et al., 2000).

3.2. PEG loading

The surface coating obtained after applying HS–PEG–COOH onto GOPTS-treated substrates was found to be reproducible. The thickness of the PEG layer increased rapidly during the first hours and reached 2.3 ± 0.2 nm after 30 h, in line with literature values for similarly deposited PEG layers (Piehler et al., 2000; Schlapak et al., 2006). Considering that the density of HS–PEG–COOH is 1.09 g/cm^3, this represents a load of 2.7 ng/nm^2 equivalent to a chain density of 0.54 molecules/nm^2. If the attachment to the surface occurred exclusively through the thiol group, one can assume a 99 pmol/cm^2 concentration of carboxy groups (Table 1). Additional characterization of the HS–PEG–COOH layer was provided by XPS analysis. Reduction of the intensity of the Si peaks and a high carbon to oxygen ratio evidences the success of the PEG coupling. The contact angles of the grafted layers were reproducible in all experiments ($32° \pm 1°$); lower than those of the GOPTS-surface and comparable to literature values.

The thickness of H_2N–PEG–NH–Boc layers was slightly higher than the thickness of HS–PEG–COOH layers, i.e. around 2.5 nm. Since the Boc-protected amino groups avoid the occurrence of any double coupling onto the chip surface we can assume an effective concentration of amino groups equal to 97 pmol/cm^2 or 0.59 molecules/nm^2 (Table 1).

In contrast, the self-assembled monolayers (SAMs) of low-molecular alkylthiols on gold, which are primarily used for surface modification of Surface Plasmon Resonance (SPR) sensors, have typically 4.8 molecules/nm^2 (Strong and Whitesides, 1998). However

Table 1
Summary of ellipsometric and contact angle data for silicon surfaces coated with GOPTS, GOPTS/HS–PEG–COOH and GOPTS/H_2N–PEG–NH_2. characterization of the surface layers: ellipsometry and contact angle measurements.

Layer	Thickness [nm]	Density [mg/ml]	Surface loading [ng/mm^2]	Chain density [molecules/nm^2]	Static contact angle [°]	Hysteresis [°]
GOPTS	1.4 ± 0.5	1.07	1.50	3.82	53 ± 2	16 ± 2
HS–PEG–COOH	2.3 ± 0.2	1.09	2.51	0.54	32 ± 1	8 ± 2
H_2N–PEG–NH_2	2.5 ± 0.2	1.09	2.73	0.59	21 ± 1	4 ± 1

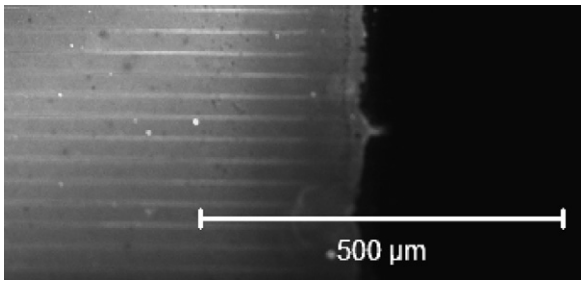

Fig. 3. Fluorescence confocal microscopy picture of a structured chip coated with H_2N–PEG–NH_2. Alexa-fluor® 555 cadaverine was applied as described in Section 3.2. The right side was covered with tape during the reactions to set the background reference level.

the optimal surface concentration of functional groups for the receptor immobilization is much lower. Particularly in the case of mixed SAMs of 16-mercapto-1-hexanoic acid (16-MHA) and 11-mercapto-1-undecanol (11-MU), the highest amount of functional receptors (Nanobodies) was immobilized on a SAM containing only 10 mol% of the acid component (Huang et al., 2005). Moreover, mixed SAM layers are generally less well packed than single-alkylthiol SAMs. Therefore the surface concentration of carboxy groups in the mixed SAMs of 16-MHA and 11-MU was less than 0.48 molecules/nm^2. Thus, the comparison of the surface concentrations of functional groups indicates that the above mentioned PEG brushes not only have the ability to reduce non-specific binding but that they also have a sufficient surface concentration of functional groups, comparable to that present in mixed SAMs used as typical sensing layers of SPR immunosensors.

After Boc-deprotection and biotinylation of the chip surface, the contact angle of the substrates was $21^\circ \pm 1^\circ$. The increased hydrophilicity indicated by static contact angle, together with the low hysteresis observed in the dynamic contact angle (4°) has been attributed to the low roughness of the layer (Piehler et al., 2000).

To verify the presence of reactive primary amino groups on the surface of the structured chips, we analyzed them by fluorescence confocal microscopy. Chips were partially covered with adhesive tape and immersed in a 2% glutaraldehyde aqueous solution for 1 h. After thorough rinsing with MilliQ water, substrates were blown dried with argon and placed on dry plates. 50 µl of a 1 mg/ml solution of Alexa-fluor® 555 cadaverine in DMF reacted for 2 h with the surface before rinsing with Milli Q water. The confocal microscopy image (Fig. 3) showed homogenous coloration over the surface of the chip, thus confirming a presence and homogeneous distribution of amino groups. To rule out the presence of adsorbed dye we examined negative control samples. No fluorescence signal was detected on samples covered with PEG but not pre-activated before applying the dye under the same reaction and cleaning conditions.

4. Optical biosensing experiments of specific and non-specific interactions

The high affinity avidin/biotin couple has been used as a model biosensing couple to demonstrate repeatability and detection capabilities of the microring resonators. Bovine Serum Albumin (BSA), a protein with similar molecular weight to avidin but with low affinity to biotin, has been used as a model for non-specific interactions. After deprotection of the Boc groups, chips coated with H_2N–PEG–NH–Boc were biotinylated and placed in the optical setup described in paragraph 2.3. PBS (10 mM $NaHPO_4$, 150 mM NaCl, pH 7.4) was used as running buffer. The signal of the chips immersed in PBS was taken as a reference level. Fig. 4 shows the response signal of the chips to a range of avidin concentrations; 2, 10, 87.5 and 175 µg/ml and two response signals of the chips to BSA solution at concentration 1 mg/ml. Every curve corresponds to a

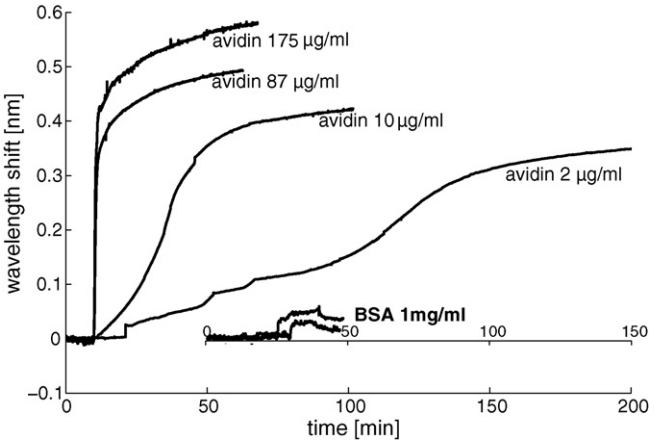

Fig. 4. Specific versus non-specific binding tests: interaction of six biotinylated H_2N–PEG–NH_2 coated chips. Wavelength shift obtained due to the interaction with avidin (2, 10, 87,5 and 175 µg/ml) and with BSA (1 mg/ml). For BSA interaction two signals on two separate chips are shown. The kink in the 2 µg/ml signal was due to a flow problem: when an air bubbles gets trapped, a short increased flow rate pushes it through.

different experiment on a different chip. For high concentrations, a fast wavelength shift is initially recorded due to the sudden concentration gradient. Then, the response increases more gradually due to the slow transport of the molecules to the surface. The lower the concentration the slower the molecular transport, which is clearly visible from the recorded data. Sensor calibration can be done either by monitoring the shift at a certain time, after a certain transported volume, or by calculating the slope of the S-curve. A calibration table can be made for various molecular interaction couples and for a broad concentration range. The kink in the 2 µg/ml signal is due to a flow problem: when an air bubble gets trapped, a short increased flow rate is needed to push it through. No shift back was observed when the chips were rinsed with PBS at the end of the experiment. This is in agreement with the specific binding of avidin, rather than its adsorption, due to the low dissociation constant of avidin/biotin and the absence of a bulk refractive index effect at these concentrations. From the saturation levels we can extrapolate a sensitivity of 10 ng/ml corresponding to the noise level of the fitted data (2 pm), which is in the same range as the sensitivity reported for the 3-aminopropyltriethoxy silane (APTES) coated microring resonators (De Vos et al., 2007). This compares well with commercially available label-free protein detection methods. We believe that further miniaturization of the flow cell for faster particle delivery will speed up the measurements.

Fig. 5 shows a comparison of the signal provided by chips with and without the PEG coating. Curve A shows the interaction of 10 µg/ml avidin with a biotinylated PEG coated chip. The response signal to avidin arises 210 times above the noise level. Curve C shows the interaction of 17 µg/ml BSA with a GOPTS covered chip. It is clear that even for this small BSA concentration, in absence of the PEG coating, a rather high output is measured. Curve B shows the signal obtained by applying increasing BSA concentrations on a PEG coated chip. For a BSA concentration of 17 µg/ml no distinguishable signal was measured, whereas for 50 µg/ml BSA the signal exceeded only 2.5 times the noise level. For a 1 mg/ml BSA concentration the response was only about 15 times the noise level, taken into account the backshift after rinsing with PBS (such high molecular concentrations cause a bulk refractive index change).

Using the vectorial mode solver software Fimmwave, we can simulate the wavelength shift for a layer surrounding the waveguide. For a wavelength shift of 2 pm, equivalent to the noise level of the fitted data, the minimal detectable thickness can be

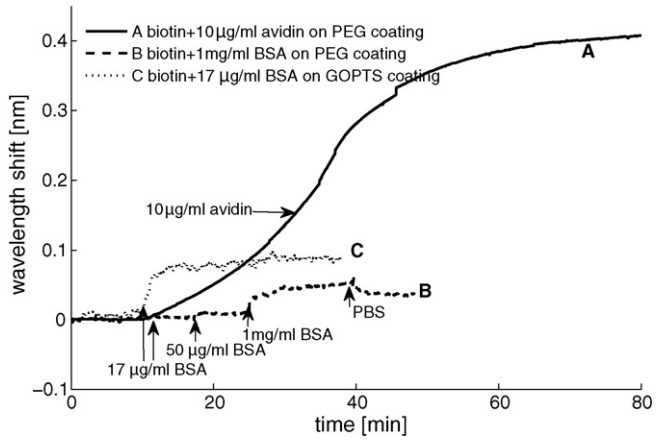

Fig. 5. Comparison of chips with and without H_2N–PEG–NH_2 coating: (A) specific interaction on a H_2N–PEG–NH_2 coated surface, (B) non-specific interaction on a H_2N–PEG–NH_2 coated surface with increasing BSA concentrations, (C) non-specific interaction on a non H_2N–PEG–NH_2 coated surface.

extracted from the simulated data. Using an approximated constant of 1.33 g/cm^3 as molecular layer mass density and a refractive index of 1.45 (Vörös, 2004), from the minimal detectable thickness of 12 fm we can estimate a minimal detectable mass coverage of about 17 pg/mm^2. As mentioned, one of the benefits of using the resonating structures rests on its small size and the fact that their response is not influenced by the sensing area. Thus, with a surface area of only 21.84 μm^2 a minimal mass of 0.37 fg could theoretically be detected.

5. Conclusions

We successfully applied a PEG coating to Silicon-on-Insulator photonic biosensor chips in order to reduce non-specific binding. A non-specific binding test revealed very low signals for BSA concentrations up to 1 mg/ml. In contrast, specific avidin detection presented a sensitivity down to 10 ng/ml, which compares well with commercially available label-free protein detection methods. Two polymer coatings were investigated and successfully applied; HS–PEG–COOH and H_2N–PEG–NH_2. In both cases, care was taken to exclude the possible attachment to the surface through both terminal groups, hence maximizing the number of reactive sites. We were able to produce thin and homogenous coatings on nanostructured surfaces that do not deteriorate the optical field sensor's intrinsic detection limit and that give a stable and reproducible signal. Applying a hydrophilic coating makes this proof-of-principle biosensor ready to be lined up in arrays and to be integrated in a microflow system for multiparameter biosensing on cheap disposable chips.

Acknowledgements

This work was funded by Ghent University through the GOA project B/05958/01 and by IAP 6-10 Photonics@be. K. De Vos thanks the Flemish Institute for the Promotion of Innovation through Science and Technology (IWT) for a specialization grant.

References

Andruzzi, L., Senaratme, W., Hexemer, A., Sheets, E.D., Ilic, B., Kramer, E.J., Baird, B., Ober, C.K., 2005. Langmuir 21, 2495–2504.
Armani, A.M., Kulkarni, R.K., Fraser, S.E., Flagan, R.C., Vahala, K.J., 2007. Science 317, 783–787.
Bluemmel, J., Perschmann, N., Aydin, D., Drinjakovic, J., Surrey, T., Lopez-Garcia, M., Kessler, H., Spatz, J.P., 2007. Biomaterials 28, 4739–4747.
Bogaerts, W., Baets, R., Dumon, P., Wiaux, V., Beckx, S., Taillaert, D., Luyssaert, B., Van Campenhout, J., Bienstman, P., Van Thourhout, D., 2005. Journal of Lightwave Technology 23 (1), 401–412.
Chao, C.Y., Guo, L.J., 2006. IEEE Journal of Selected Topics in Quantum Electronics 12, 134–142.
Densmore, A., Xu, D.-X., Janz, S., Waldron, P., Lapointe, J., Mischki, T., Lopinski, G., Delâge, A., Schmid, J.H., Cheben, P., 2008. Advances in Optical Technologies, 725967–725976.
De Vos, K., Bartolozzi, I., Schacht, E., Bienstman, P., Baets, R., 2007. Optics Express 15, 710–715.
Fan, X., White, I.M., Shopova, S.I., Zhu, H., Suter, J.D., Sun, Y., 2008. Analytica Chimica Acta 620, 8–26.
Herzinger, C.M., Johs, B., McGahan, W.A., Woollam, J.A., Paulson, W., 1998. Journal of Applied Physics 83, 3323–3336.
Huang, L., Reekmans, F., Saerens, D., Friedt, J.M., Frederix, F., Francis, L., Muyldermans, S., Campitelli, A., Hoof, C.V., 2005. Biosensors and Bioelectronics 21, 483–490.
Luzinov, I., Julthongpiput, D., Liebmann-Vinson, A., Cregger, T., Foster, M.D., Tsukruk, V.V., 2000. Langmuir 16, 504–516.
Moerner, W.E., 2007. Proceedings of the National Academy of Science 104, 12596–12602.
Norde, W., Gage, D., 2004. Langmuir 20, 4162–4167.
Piehler, J., Brecht, A., Valiokas, R., Liedberg, B., Gauglitz, G., 2000. Biosensors and Bioelectronics 15, 473–481.
Proll, B., Mohrle, S.K., Kumph, M., Gauglitz, G., 2005. Analytical and Bioanalytical Chemistry 20, 6727–6735.
Ramachandran, A., Wang, S., Clarke, J., Ja, S.J., Goad, D., Wald, L., Flood, E.M., Knobbe, E., Hryniewicz, J.V., Chu, S.T., Gill, D., Chen, W., King, O., Little, B.E., 2008. Biosensors and Bioelectronics 23, 939–944.
Schlapak, R., Pammer, P., Armitage, D., Zhu, R., Hiterdorfer, P., Vaupel, M., Fruhwirth, T., Howeorka, S., 2006. Langmuir 22, 277–285.
Selvaraja, S., Bogaerts, W., Van Thourhout, D., Baets, R., 2008. 14th European Conference on Integrated Optics (ECIO), Netherlands.
Strong, L., Whitesides, G.M., 1998. Langmuir 4, 546–558.
Tompkins, H.G., McGahan, W.A., 1999. Spectroscopic Ellipsometry and Reflectometry, 1st ed. J. Wiley & Sons Incorporation.
Unsworth, L.D., Sheardown, H., Brash, J.L., 2007. Langmuir 24, 1924–1929.
Vollmer, F., Arnold, S., 2008. Nature Methods 5 (7), 591-506.
Vörös, J., 2004. Biophysical Journal 87, 553–561.
White, I.M., Fan, X., 2008. Optics Express 16 (2), 1020–1028.
Wolter, A., Niessner, R., Seidel, M., 2007. Analytical Chemistry 79, 4529–4537.
Yu, X., Xu, D., Cheng, Q., 2006. Proteomics 6 (20), 5493–5503.